Applied Food Research 5 (2025) 100969

Contents lists available at ScienceDirect

Applied Food Research

journal homepage: www.elsevier.com/locate/afres

Tailoring the functional properties of *Jir* starch from pearl millet: Effects of extraction layer, fermentation time, and sudanese genotypes

Manhal Gobara Hamid [a,c], Khitma A. Sir Elkhatim [a,c], Amro B. Hassan [b], Mohamed A Ibraheem [b], Yousif M.A. Idris [c], Faraz Muneer [4], Mohammed Elsafy [d,*], Mahbubjon Rahmatov [d], Eva Johansson [d], Tilal Abdelhalim [a,*]

[a] Biotechnology and Biosafety Research Center, Agricultural Research Corporation, Shambat, Khartoum North, Sudan
[b] Department of Food Science and Nutrition, College of Food and Agricultural Sciences, King Saud University, PO Box 2460, Riyadh 11451, Saudi Arabia
[c] College of Agricultural Studies, Sudan University of Science and Technology, Shambat, Khartoum North, Sudan
[d] Department of Plant Breeding, Swedish University of Agricultural Sciences (SLU), PO Box 190 234 22, Alnarp, Sweden

ARTICLE INFO

Keywords:
Functional properties
Fermentation
Indigenous food
Pearl millet
Starch

ABSTRACT

This study investigated the potential of *Jir*, a starch derived from fermented dehulled pearl millet grains, and its future applications. The physicochemical, colorimetric, thermal, pasting, and textural properties of *Jir* were evaluated across five Sudanese pearl millet genotypes, two extraction layers, and two fermentation durations. Principal component analysis (PCA) and partial least squares (PLS) regression showed that the extraction layer had a greater influence on starch properties than the genotype or fermentation duration. Colorimetric and pasting properties were crucial for distinguishing the layers, with the lower layer showing significantly higher lightness (L*), whitening index (WI), peak viscosity, and final viscosity than the upper layer. After seven days of fermentation, PLS identified the lower layer of the Bioda genotype as the most suitable starch source for traditional Sudanese porridge. ANOVA, PCA, and PLS analyses revealed multiple interactions between genotype, extraction layer, and fermentation duration, suggesting opportunities to optimize *Jir* properties through careful selection of raw materials and fermentation processes. This optimization can create new starch-based ingredients with enhanced nutritional qualities, offering diverse applications in the food industry and supporting innovation in indigenous products.

1. Introduction

Pearl millet (*Pennisetum glaucum* L. R. Br. syn. *Cenchrus americanus* L. Morrone) is a climate-resilient crop that plays a vital role in ensuring food security due to its exceptional nutritional value (Tonapi et al., 2024). Globally, it is a staple for more than 90 million people, particularly in arid and semi-arid regions (Serba et al., 2020). Naturally gluten-free, pearl millet is suitable for individuals with celiac disease or gluten intolerance (Yousaf et al., 2021). Its grains are rich in essential nutrients, containing approximately 14.0 % proteins (14.0 %), 63.2 % starch, 2.8 % dietary fibers (both soluble and insoluble), 2.1 % ash, and substantial micronutrients, minerals, and antioxidants (Ali et al., 2003; Elsafy et al., 2024). As such, incorporating pearl millet into daily diets and food products holds great potential for improving nutritional quality, particularly in communities affected by micronutrient deficiencies and malnutrition.

In Sudan, pearl millet, locally known as dukun, is the primary dietary energy and protein source for much of the Western Sudanese population (Abdalla et al., 1998). The grains are central to a variety of traditional dishes, including *Balila* (boiled grains), *Kisra* (fermented or unfermented pancakes), *Aseda* (stiff porridge) or *Nasha* (thin gruel), *Madida* (thin porridge cooked with natron), and beverages such as the local alcoholic brew *Marisa* and its non-alcoholic counterparts *Abrei* or *Hullu-murr* (Elsafy et al., 2024).

A particularly distinctive product is Jir, a highly refined starch extracted through the spontaneous fermentation of dehulled pearl millet grains (Dirar, 1993), characterized by its jelly-like quivering consistency and nearly translucent, lump-free texture. Due to its smooth, consistent texture and chalk-like appearance, Jir is initially referred to as the lime or whiting used for whitewashing buildings. In the Darfur region, Jir

* Corresponding authors.
E-mail addresses: mohammed.elsafy@slu.se (M. Elsafy), tilalkosti@yahoo.com (T. Abdelhalim).

https://doi.org/10.1016/j.afres.2025.100969
Received 21 October 2024; Received in revised form 20 April 2025; Accepted 15 May 2025
Available online 16 May 2025
2772-5022/© 2025 The Author(s). Published by Elsevier B.V. This is an open access article under the CC BY license (http://creativecommons.org/licenses/by/4.0/).

holds significant cultural value, which is especially prepared for weddings and ceremonies served to guests, celebrities, dignitaries, and VIPs. Women from the Fur tribe are especially renowned for their artisanal expertise in producing high-quality Jir (Dirar, 1993, 1994).

Jir production is a deeply rooted tradition in Sudanese culture, with preparation techniques meticulously passed down through generations, particularly among women within families. This starch-rich food holds profound cultural significance, symbolizing hospitality, respect, and social status. Beyond its ceremonial role, Jir-making embodies an essential vehicle for intergenerational knowledge transfer and the preservation of culinary craftsmanship (Dirar, 1993, 1994). While Jir has not traditionally been produced commercially, it holds strong potential as an artisanal food product that could empower women and contribute to rural economic development. However, the rising preference for industrial starch products threatens this indigenous practice. This growing shift highlights the urgent need to document, safeguard, and promote Jir-making as an essential element of Sudan's food heritage and cultural identity (Dirar, 1993, 1994).

The preparation of Jir begins with fermenting dehulled pearl millet grains in a large traditional earthenware jar, locally known as a *zeer*, for a duration ranging from 1 to 14 days. This spontaneous fermentation process involves complex microbial succession, primarily driven by lactic acid bacteria (LAB) and yeast communities. LAB, particularly species from the genus *Pediococcus*, predominates during the early stages of fermentation, while yeast species become more prominent in the later stages (Samah & Muna, 2011). Key yeast species regulating Jir fermentation include *Schizosaccharomyces pombe, Saccharomycods sinensis*, and *Trichosporon adeninovorans* (Zhao et al., 2019). The souring process, catalyzed by lactic acid fermentation, is critical for breaking down the protein matrix that encases starch granules in pearl millet grains, facilitating starch release (Dirar, 1993, 1994). Following fermentation, the grains are sun-dried, pounded into flour, and mixed with water to create a milk-like suspension. This mixture then isolates and separates the refined starch layers that constitute Jir (Hamid et al., 2025).

Starch isolation from various crop sources, whether through spontaneous fermentation or conventional chemical treatments, significantly influences the physicochemical properties of the extracted starch (Abdalla et al., 2009; Ali et al., 2003; Bian et al., 2022; Chandrasekar et al., 2022; Correia et al., 2013). In particular, the natural fermentation of grains has been shown to reduce antinutritional compounds such as tannins and phytates, thereby enhancing the digestibility profile of pearl millet starch (Gupta & Gaur, 2024a). However, to harness Jir's full potential for commercial and industrial applications, it is essential to standardize its traditional fermentation process. This requires a thorough understanding of how fermentation alters the starch's physicochemical properties, ultimately determining its functionality across diverse food systems.

Our previous study investigated the impact of fermentation time on the in vitro digestibility of Jir extracted from pearl millet cultivars. The results revealed that extended fermentation led to notable alterations in starch granule morphology, such as surface perforations, indentations, and structural degradation, which collectively enhanced starch digestability (Hamid et al., 2025). However, to support the broader application of Jir in food systems, a more comprehensive understanding of its fundamental physicochemical attributes of extracted starch layers, including their thermal behavior, pasting properties, and textural profiles, using five Sudanese pearl millet genotypes, is needed.

These findings will provide valuable insights into optimizing Jir for diverse food formulations, improving its shelf life, and maximizing its nutritional and functional benefits. Ultimately, these results are vital for advancing the commercialization and large-scale production of Jir and other traditional starch-based products

2. Materials and methods

2.1. Plant materials

Four Sudanese pearl millet genotypes and one released cultivar were used in this study. The released cultivar Ashana is known for its resistance to downy mildew, early maturation, and high grain yield. The pearl millet genotypes were Bioda, Demi-green, Dembi-red, and Mayoa. Bioda, a white pearl millet preferred by farmers, is commonly consumed as porridge with milk and is notable for its resistance to the white borer (*Salura infecta*). Dembi-green, Dembi-red, and Mayoa are traditional pearl millet genotypes regarded as superior in Western Sudan. All five pearl millet genotypes were obtained from the Nayala Research Station of the Agricultural Research Corporation (ARC) in Sudan.

2.2. Jir preparation

The traditional starch extraction (Jir) process from five Sudanese pearl millet genotypes was carried out by two expert women from the Darfur region, following the procedures described by Dirar (1993), with slight modifications. Initially, the pearl millet grains were cleaned to remove dirt and stones and then winnowed in a customary flat basket called a *Tabak* (Fig. 1). The cleaned grains were manually dehulled using a traditional wooden pestle and mortar, followed by sun-drying for approximately three hours under ambient conditions (average temperature:33 °C; relative humidity: ~30 %).

The dehulled grains were soaked in water in a clean plastic container and left to undergo natural fermentation at room temperature for 1 or 7 days. During the 7-day fermentation, approximately 25-30 % of the surface water was replenished every three days to maintain microbial activity and ensure proper submersion. The water-to-flour ratio was maintained at 3:1, submerging the grains with an additional 2-3 cm of water above the surface.

After fermentation, the grains were sieved, sun-dried in a dust-free, well-ventilated area for 6-7 hours, and ground into a fine flour using traditional tools. The flour was mixed with water to form a milk-like suspension, which was sieved using a fine mesh filter and allowed to settle overnight. The sedimented mixture was then mashed, reconstituted in water, and sieved up to three times to extract the maximum amount of starch. Following the final sieving, the starch-rich suspension was stirred for 30 minutes using a clean wooden stirrer, covered tightly, and left undisturbed overnight. By morning, the starchy material had settled. The supernatant water was gently decanted using a half gourd (Kass) to preserve the underlying sediment. Based on visual inspection and tactile consistency, the starch sediment was separated into two distinct layers: *Jir Khadim* (the upper, loose, slightly discolored layer)

Fig. 1. A customary flat basket called a *Tabak*.

and *Jir Hur* (the lower, white, firm, and cohesive layer). These layers were distinguished by the experienced women based on color and texture.

Each layer was carefully transferred using a Kass, spread onto aluminum trays, and sun-dried at 30–35 °C for approximately 8 hours. Periodic stirring ensured uniform drying. Once completely dry, the starch from each layer was collected and stored separately for subsequent physicochemical analyses (Fig. 2).

2.3. Measurements of the physicochemical properties

2.3.1. Amylose content

The amylose content of the pearl millet starch *Jir* was assessed using a rapid calorimetric method. To prepare the standard, 40 mg of potato

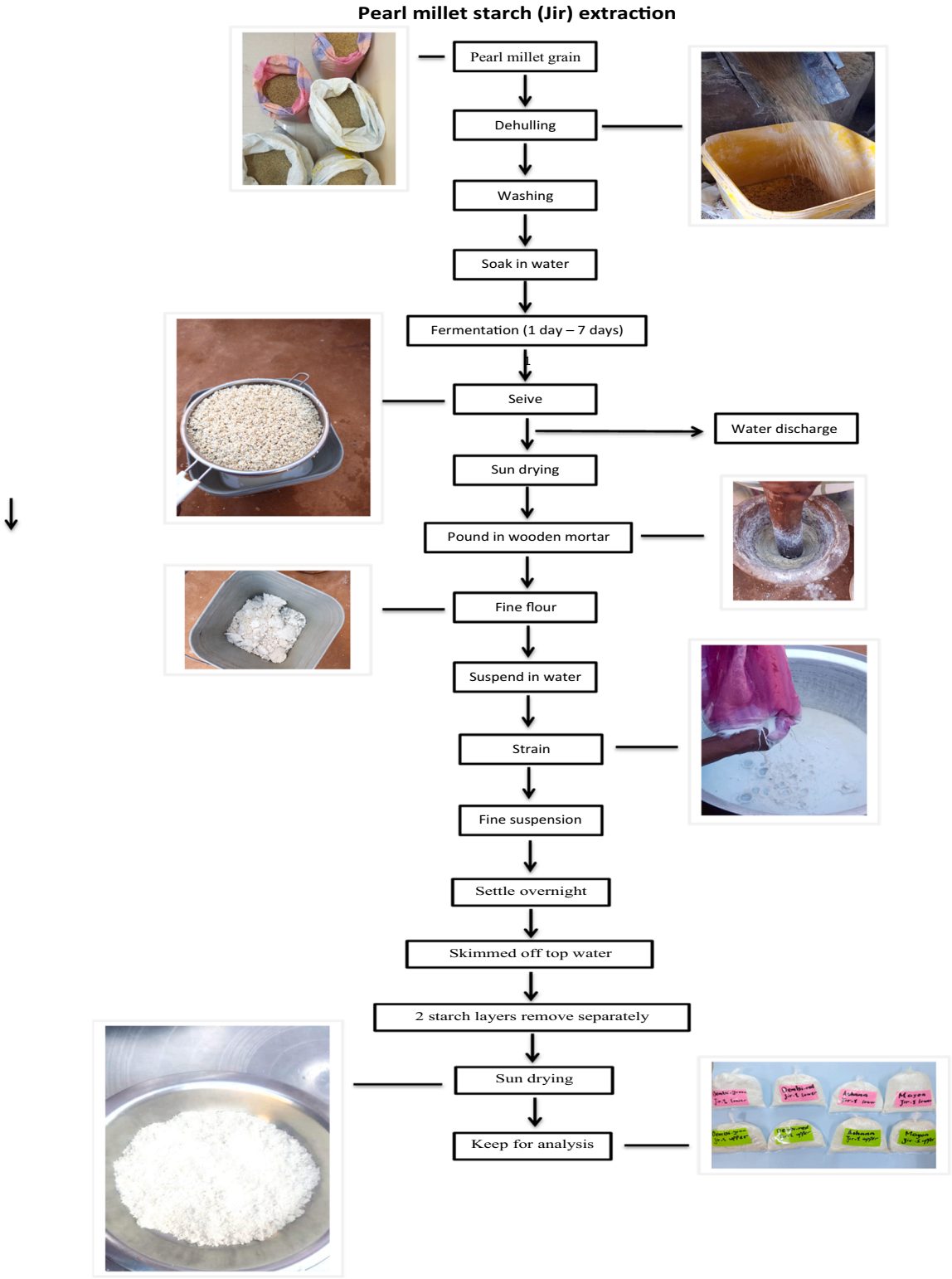

Fig. 2. Flowchart depicting the Jir preparation.

starch (containing amylose) was added to 100 mL of standard starch solution. Then, 1 ml of 95 % ethanol and 9.0 ml of 1 N NaOH were added. The mixture was thoroughly agitated and boiled in a water bath for 10 min before being diluted to 100 ml. A standard amylose curve was constructed following the method described by Juliano (1971). For sample preparation, 100 mg of pearl millet starch *Jir* was weighed into a 100 ml volumetric flask, and 1 ml of 95 % ethanol and 9 ml of 1 N NaOH were added. The starch solutions were then boiled in a water bath for 10 min, cooled to room temperature, and diluted to 100 ml. (Williams, 1970). For amylose determination, 10 μL of starch solution, 200 μL of 1 N acetic acid, and 10 μL of iodine solution (0.2 % I and 2.0 % KI in distilled water) were pipetted into the microplate wells. The mixture was vortexed twice for 30 s, and once again every 4 min before measuring absorbance. Absorbance was measured after 5 min at 620 nm using a Thermo Scientific Multiskan Go microplate spectrophotometer. The amylose content of the pearl millet starch *Jir* samples was expressed as a percentage relative to the standard curve (Cobb & Schoelles, 1989).

2.3.2. Damaged starch

Starch damage in the *Jir* samples was quantified using the rapid non-enzymatic method described by McDermott (1980). A mixture of trichloroacetic acid (TCA; 10 g in 300 ml distilled water) and potassium thiocyanate (KSCN; 30 g in 300 ml distilled water) was prepared at a 1:1 ratio. Next, 50 g of the starch sample was combined with 20 ml of the TCA-KSCN mixture and incubated in a water bath at 30 °C for 15 min. The samples were then processed using an ultrasonic extractor for 5 min, followed by additional incubation in a water bath at 30°C with agitation using a shaker for 15 min.

The resulting suspension was filtered into a test tube, and 1 ml of iodine solution (0.2 g iodine crystal and 2 g potassium iodide in 100 ml distilled water) was added to the filtrate, producing a blueish-green color. The mixture was then incubated in a water bath at 21 °C for 10 min. Color density was measured using a Thermo Scientific Multiskan Go microplate spectrophotometer at 600 nm. The extent of starch damage was expressed in Farrand units (FUs).

The Farrand units (FU) were calculated using the following formula:

$$FU = OD \times 0.97 + 2.1$$

where OD is the optical density of the filtrate (2.0 ml of filtrate and 0.50 g of flour).

2.3.3. Water absorption capacity (WAC)

The water absorption capacity (WAC) of the extracted *Jir* samples was assessed following the protocol established by Lin and Zayas (1987), with slight modifications. Briefly, 1 g of *Jir* was mixed with 10 ml of distilled water in a pre-weighed centrifuge tube and allowed to equilibrate for 1 h at room temperature. The mixture was then centrifuged at 1500 G for 30 min. After centrifugation, the supernatant was carefully decanted, and any remaining water droplets were removed from the tube. The tube was then weighed again to determine the weight of the retained water. The weight (g) of water retained in the sample was recorded as the WAC.

2.3.4. Bulk density (BD)

Bulk density (BD) was assessed using the method described by Wang and Kinsella (1976). Briefly, 10 g of the extracted *Jir* sample was placed in a 50 ml graduated cylinder. The cylinder was gently tapped on the bench top ten times to allow the sample to settle uniformly. The final sample volume of the sample was then recorded. The BD was calculated and expressed in grams al per cubic centimeter (g/cm^3).

2.4. Color measurement

Color analysis of the traditionally extracted *Jir* was conducted using a JZ-300 general colorimeter. The starch samples were scanned thrice to obtain the average L* (lightness), a* (redness/greenness), and b* (yellowness/ blueness) values. The Whiteness Index (WI) was calculated followed the method described by Alegria et al. (2012).The Total Color Difference (ΔE*) relative to corn starch was calculated using the methodology described by Maskan (2001). The calculations were performed using the following formula:

$$\Delta E = \sqrt{\Delta a^{*2} + \Delta b^{*2} + \Delta L^{*2}}$$

$$WI = 100 - \sqrt{(100 - L^{*})^2 + a^{*2} + b^{*2}}$$

These indices provide a quantitative measure of the color attributes and deviations of pearl millet starch compared to a standard reference.

2.5. Thermal properties

The thermal properties of the *Jir* samples were investigated using a Differential Scanning Calorimetry (DSC) instrument (Q 2000, TA Instruments, USA). Samples (6–8 mg) were mixed with 10 μL of distilled water in hermetically sealed aluminum pans and equilibrated at room temperature for three hours. An empty pan was used as a reference. Thermal scanning was performed from 30°C to 120°C at a heating rate of 10°C/min. Key thermal parameters, including the enthalpy of gelatinization (ΔH, J/g), onset temperature (T0), and peak temperature (PT), were analyzed using the Universal Analysis software.

2.6. Pasting properties

The pasting properties of *Jir* starches were analyzed using a Rapid Visco Analyzer (RVA) (Newport Scientific, Sydney, Australia). For the analysis, 2 g of starch (adjusted to 14 % moisture) was weighed in aluminum canisters, and the total weight was 28 g by adding the distilled water. The RVA test followed a temperature profile that included an initial holding step at 50°C for 30 s, a linear temperature increase to 95°C at a rate of 10.23 °C/min, a holding step at 95°C for 4 min, a linear temperature decrease to 50°C at 22.5°C/min, and a final isothermal step at 50°C for 2 min. The paddle speed was initially set to 960 rpm for 10 s, and then decreased to 160 rpm for the remainder of the test. The measured RVA parameters included peak temperature, breakdown, final temperature, and setback viscosity. Data were analyzed using Thermocline for Windows software (Newport Scientific, Warriwood, NSW2102, Australia).

2.7. Gel Texture

The gel texture parameters were assessed using gels prepared with the Rapd Visco Analyzer (RVA). The gels were transferred into 25 mL beakers (35 mm in height) with an internal diameter of 30 mm and stored overnight at room temperature. Compression tests were then performed on the gels using a Brookfield CT3 Texture Analyzer (Brookfield Engineering Laboratories, Inc., Middleboro, USA). The tests involved two penetration cycles at a speed of 0.5 mm /s to a distance of 10 mm , using a cylindrical probe measuring 12.7 mm in diameter and 35 mm in high. The gel hardness, springiness, cohesiveness, and adhesiveness were recorded directly from the instrument.

2.8. Statistical analysis

Data were tested for homogeneity of variance and normality using Levene's test and Shapiro-Wilk's test, respectively, with a significance level set at $P < 0.05$. The effects of pearl millet genotypes, fermentation time, and *Jir* extraction layers, and their interactions were analyzed using three-way ANOVA with XLSTAT software (Vidal et al., 2020). The Tukey HSD post hoc test was applied to treatments with significant differences for further analysis. Multivariate analysis was conducted using Principal Component Analysis (PCA), Correlation plots and Partial

Least Squares Regression (PLS) were generated using the *prcomp* function in R, and visulalizations were created using the *factoextra, pls, ggcorrplot, ggplot2*, and *ggrepel* packages. The final model for Partial Least Squares (PLS) Regression was:

$$Y = XW(BQ) + F$$

Where: **X** is the matrix of predictors that includes variables such as fermentation days, extraction layer, and physicochemical properties such as bulk density, peak viscosity, and amylose content., **W** is the matrix of weights that transforms the original predictors into latent variables (scores) that maximize the covariance between *X* and the response *Y*.,

B is the diagonal matrix of regression coefficients representing the strength of the relationship between these latent variables and the response *Y*., **Q** is the matrix of loadings for *Y* indicating how each response variable, such as the quality attributes, is associated with the latent variables derived from *X*., **F** represents the residuals, capturing the variation in *Y* that is not explained by the model.

3. Results

3.1. Physicochemical characters

Physicochemical characteristics of the extracted pearl millet starch *Jir*, revealed significant (P<0.05) differences in amylose content, bulk density, water absorption capacity, and damaged starch content across genotypes, fermentation times, and extraction layers. The interactions between these functional properties were also significant (P<0.05) (Table 1). Seven days of fermentation resulted in higher bulk density, water absorption capacity, and starch damage compared to one day of fermentation; however, amylose content did not follow the same trend.

Table 1
Amylose content (%), bulk density (g/cm3), water absorption capacity (ml/g), and damaged starch (BV) of extracted starch "Jir" from dehulled pearl millet grains as influenced by pearl millet genotypes, fermentation time, extraction layers, and their possible interactions.

Genotypes	Physiochemical properties			
	Amylose content (%)	Bulk Density (g/cm^3)	Water absorption capacity (ml/g)	Damaged starch (BV)
Ashana	17.96 ($\pm$1.3)^{A}	4.03 ($\pm$0.12)^{B}	0.93 ($\pm$0.03)^{BC}	3.00 ($\pm$0.02)^{BC}
Bioda	17.93 ($\pm$1.5)^{A}	3.87 ($\pm$0.17)^{D}	1.13 ($\pm$0.10)^{A}	3.20 ($\pm$0.09)^{A}
Dembi-green	16.61 ($\pm$1.1)^{B}	3.98 ($\pm$0.12)^{BC}	1.04 ($\pm$0.03)^{AB}	3.11 ($\pm$0.03)^{AB}
Dembi-red	16.92 ($\pm$0.8)^{B}	3.88 ($\pm$0.10)^{CD}	1.07 ($\pm$0.02)^{AB}	3.14 ($\pm$0.02)^{A}
Mayoa	15.69 ($\pm$0.8)^{C}	4.15 ($\pm$0.10)^{A}	0.92 ($\pm$0.02)^{C}	2.99 ($\pm$0.02)^{C}
Fermentation periods				
1 Day	20.06 ($\pm$0.5)^{A}	3.91 ($\pm$0.05)^{B}	0.97 ($\pm$0.02)^{B}	3.05 ($\pm$0.02)^{B}
7 days	13.98 ($\pm$0.2)^{B}	4.06 ($\pm$0.10)^{A}	1.06 ($\pm$0.04)^{A}	3.13 ($\pm$0.04)^{A}
Extraction layers				
Lower	18.02 ($\pm$0.8)^{A}	4.26 ($\pm$0.07)^{A}	1.06 ($\pm$0.04)^{A}	3.12 ($\pm$0.04)^{A}
Upper	16.03 ($\pm$0.5)^{B}	3.71 ($\pm$0.04)^{B}	0.98 ($\pm$0.02)^{B}	3.05 ($\pm$0.02)^{B}
Three-Way ANOVA				
Genotypes, G	46.0***	16.2***	11.8***	11.8***
Fermentation, F	2334.2***	35.3***	14.1***	14.1***
Layers, L	250.6***	459.3***	9.7**	9.7**
G*F	114.7***	16.4***	3.4*	3.4*
G*L	25.0***	25.4***	10.7***	10.7***
F*L	329.4***	264.6***	14.7***	14.7***
G*F*L	14.6***	8.8***	12.4***	12.4***

The lower layer (*Jir Hur*), exhibited significantly (P<0.05) higher amylose content, bulk density, water absorption, and starch damage than the upper layer (*Jir Khadim*) (Table 1).

The highest amylose content was observed in *Jir* starch extracted from Ashana and Bioda genotypes, both at 18 %, which was significantly (P<0.05) higher than the amylose content of the other genotypes. Conversely, *Jir* starch extracted from Mayoa had the lowest amylose content among the varieties examined. No significant (P<0.05) difference was found in amylose content between the Dembi-green and Dembi-red genotypes. Mayoa exhibited the highest bulk density of *Jir* among the pearl millet genotypes. In contrast, the Bioda and Dembi-red genotypes had the lowest *Jir* bulk densities. Water absorption capacity and damaged starch followed a consistent pattern, with Bioda and Dembi-red showing the highest values, whereas Mayoa displayed the lowest values (Table 1).

For the effect sizes the regarding amylose (%), fermentation periods showed the most significant effect on amylose content ($\eta^2 = 0.605$; partial $\eta^2 = 0.984$; Cohen's f = 7.800), followed by pearl millet genotypes ($\eta^2 = 0.065$; Cohen's f = 2.555) and extraction layers ($\eta^2 = 0.064$; Cohen's f = 2.541). The interaction of genotype × fermentation periods ($\eta^2 = 0.135$) and fermentation periods × extraction layers ($\eta^2 = 0.084$) also contributed significantly, while all other interactions exhibited minimal effects (Table S1).

The extraction layers had the highest effect on bulk density ($\eta^2 = 0.427$; partial $\eta^2 = 0.919$; Cohen's f = 3.374), followed by fermentation periods × extraction layer ($\eta^2 = 0.254$; Cohen's f = 2.600), and pearl millet genotypes × extraction layers ($\eta^2 = 0.097$; Cohen's f = 1.610). Pearl millet genotypes and fermentation periods alone contributed smaller effect sizes (Table S1).

Genotype was the most influential factor for water absorption capacity (WAC) ($\eta^2 = 0.206$; Cohen's f = 1.096), followed closely by the interaction of fgenotypes × extraction layers ($\eta^2 = 0.188$; Cohen's f = 1.047) and genotype × fermentation periods × extraction layers ($\eta^2 = 0.203$; Cohen's f = 1.089). In contrast, other interactions and single factors showed moderate to minor effects (Table S1).

The pattern for damaged starch mirrored that of WAC. Genotype ($\eta^2 = 0.206$), genotype × fermentation periods × extraction layer ($\eta^2 = 0.203$), and genotype × extraction layers ($\eta^2 = 0.188$) were the most prominent factors, with comparable partial η^2 and Cohen's f values across these effects (Table S1).

3.2. Color measurements

Quantifiable colorimetric parameters, including L*, a*, and b*, total color difference (ΔE), and whitening index (WI), showed significant (P<0.05) variations across pearl millet genotypes, fermentation durations, and extraction layers. Except for the interaction between fermentation duration and extraction layers for L*, b*, and ΔE, all other possible interactions among the factors assessed were significantly (P<0.05) different. After seven-days of fermentation, both the brightness (L*) and WI values significantly (P<0.05) increased compared to the one-day fermentation (Table 2). Conversely, the one-day fermentation period resulted in a significantly (P<0.05) higher a*, b*, and ΔE values than the seven-day fermentation. Furthermore, the lower layer of *Jir* exhibited significantly (P<0.05) higher colorimetric values than the upper layer, with the exception of b*.

The Data were evaluated using a three-way ANOVA, and the factors were five pearl millet genotypes, fermentation time, and extraction layers. According to Tukey's HSD, means values with identical letters do not differ significantly at $p < 0.05$. Asterisks (*) indicate significantly influential factors, such as ns, but they are insignificant. **significant at $p \leq 0.01$.*** significance level at $p \leq 0.001$. Each value is the average of three replicates. Data in parentheses are the standard error of means.

Among the pearl millet genotypes, Dembi-red showed the highest lightness (L*). There were no significant (P<0.05) differences in L* between the Dembi-red, Bioda, and Ashana groups (Table 2). However,

Table 2
Lightness (L*), redness/greenness (a*), yellowness/blueness (b*), total color differences (ΔE), and whitening index (WI) of extracted starch "Jir" from dehulled pearl millet grains as influenced by pearl millet genotypes, fermentation time, extraction layer, and their possible interactions.

	Color measurements of the extracted pearl millet starch *Jir*				
Genotypes	(L*)	(a*)	(b*)	(ΔE)	(WI)
Ashana	96.4 (±0.6)^{AB}	0.48 (±0.06)^{C}	8.3 (±0.6)^{AB}	7.2 (±0.2)^{AB}	94.5 (±0.4)^{B}
Bioda	96.7 (±1.0)^{AB}	1.03 (±0.23)^{A}	7.3 (±0.8)^{B}	7.5 (±0.7)^{A}	94.6 (±0.5)^{B}
Dembi-green	95.3 (±0.6)^{B}	0.93 (±0.08)^{AB}	9.5 (±0.5)^{A}	7.4 (±0.3)^{A}	93.4 (±0.4)^{C}
Dembi-red	97.3 (±0.5)^{A}	0.53 (±0.07)^{C}	7.8 (±0.4)^{B}	7.3 (±0.2)^{A}	95.0 (±0.3)^{A}
Mayoa	95.3 (±0.1)^{B}	0.58 (±0.07)^{BC}	8.0 (±0.4)^{AB}	6.8 (±0.2)^{B}	94.6 (±0.3)^{B}
Fermentation periods					
1 Day	95.6 (±0.5)^{B}	0.84 (±0.10)^{A}	8.6 (±0.4)^{A}	7.4 (±0.3)^{A}	93.9 (±0.3)^{B}
7 Days	96.8 (±0.4)^{A}	0.58 (±0.05)^{B}	7.7 (±0.3)^{B}	7.1 (±0.2)^{B}	94.9 (±0.2)^{A}
Extraction layers					
Lower	97.8 (±0.4)^{A}	0.70 (±0.11)^{A}	7.2 (±0.4)^{B}	7.8 (±0.2)^{A}	95.1 (±0.3)^{A}
Upper	94.7 (±0.4)^{B}	0.72 (±0.05)^{A}	9.2 (±0.2)^{A}	6.7 (±0.2)^{B}	93.7 (±0.2)^{B}
Three-Way ANOVA					
Genotypes, G	37.8***	111.5***	122.2***	8.4***	136.6***
Fermentation, F	85.6***	152.2***	174.0***	8.3**	429.6***
Layers, L	587.3***	0.6^{NS}	876.5***	153.2***	839.7***
G*F	55.5***	25.6***	120.5***	37.6***	108.9***
G*L	,	83.5***	54.2***	79.7***	94.2***
F*L	0.01^{NS}	68.5***	2.4^{NS}	1.9 ^{NS}	11.1**
G*F*L	80.0***	168.6***	305.2***	48.8***	319.8***

for a*, the Bioda genotype recorded the highest value (1.3), followed by Dembi-green (0.93), significantly (P<0.05) different from the values for Ashana, Dembi-red, and Mayoa. Furthermore, Dembi-green displayed the highest b* value (9.5), followed by Ashana (8.3) and Mayoa. The *Jir* extract from the Bioda genotype had the lowest b* value. Furthermore, Mayoa had a significantly (P<0.05) lower ΔE than the other four pearl millet genotypes. Among the genotypes, Dembi-red had the highest whitening index (WI). The Ashana, Bioda, and Dembi-red genotypes had similar WI values, while the Demibi-green genotype had the lowest WI.

For the effect sizes the concerning the lightness (L*), extraction layers had the largest effect ($\eta^2 = 0.330$; Cohen's f = 3.692), followed by pearl millet genotypes × extraction layers ($\eta^2 = 0.181$; Cohen's f = 2.735), and the three-way interactions genotypes × fermentation periods × extraction layers ($\eta^2 = 0.193$; Cohen's f = 2.820). Genotype ($\eta^2 = 0.085$) and fermentation periods ($\eta^2 = 0.064$) showed moderate effects, while the fermentation periods × extractions layer interaction was negligible ($\eta^2 = 0.000$) (Table S2).

Regarding the red-green axis (a*), pearl millet genotypes were the dominant factor ($\eta^2 = 0.224$; Cohen's f = 3.008), with substantial contributions from genotypes × fermentation periods × extraction layers ($\eta^2 = 0.417$; Cohen's f = 4.110), and genotypes × extraction layer ($\eta^2 = 0.167$; Cohen's f = 2.602). However, other effects were minor (Table S2).

Regarding the yellow-blue axis (b*), extraction layers had the most substantial impact ($\eta^2 = 0.271$; Cohen's f = 5.045), followed by the three-way interaction genotypes × fermentation periods × extraction layers ($\eta^2 = 0.333$; Cohen's f = 5.588), and genotypes × fermentation periods ($\eta^2 = 0.132$; Cohen's f = 3.524). Genotype ($\eta^2 = 0.153$) also showed a notable effect, while the two-way interaction of fermentation periods × extraction layers had no meaningful influence ($\eta^2 = 0.000$) (Table S2).

Pearl millet genotypes × extraction layers had the highest effect on total color difference ($\eta^2 = 0.336$; Cohen's f = 2.605), followed by the two-way interactions of pearl millet genotype × fermentation periods ($\eta^2 = 0.187$) and the three-way interaction genotypes × fermentation periods × extraction layer ($\eta^2 = 0.234$). Other factors contributed less significantly (Table S2).

For the whiteness index (WI), the three-way interaction pearl millet genotypes × fermentation periods × extraction layers showed the most decisive influence on WI ($\eta^2 = 0.314$; Cohen's f = 5.898), followed by extraction layers ($\eta^2 = 0.231$; Cohen's f = 5.058), and pearl millet genotypes ($\eta^2 = 0.145$; Cohen's f = 4.007). However, the two-way interaction of fermentation periods × extraction layer had minimal effect ($\eta^2 = 0.001$) (Table S2).

The Data were evaluated using three-way ANOVA, and the factors were five pearl millet genotypes, fermentation time, and extraction layers. Means with identical letters indicate that the values do not differ significantly at $p < 0.05$, according to Tukey's HSD. Asterisks (*) indicate significantly influential factors as ns, but they are insignificant. **significant at $p \leq 0.01$.*** significant at $p \leq 0.001$ level. Each value is the average of three replicates. Data in parentheses are the standard error of means.

3.3. Thermal properties

The study revealed no substantial variations in thermal properties, including onset temperature, peak temperature, and enthalpy, among *Jir* starch extracted from Sudanese pearl millet genotypes (Table 3). After seven days of fermentation, the onset temperature was higher than that observed after one day, although no significant (P<0.05) differences were found in peak temperatures or enthalpies. The upper layer of the extracted pearl millet starch *Jir* exhibited significantly (P<0.05) higher onset and peak temperatures than the lower layer, with no significant (P<0.05) differences in enthalpy between the layers (Table 3). Two-way interactions between pearl millet genotypes and fermentation duration and between genotypes and layers were significant (P<0.05) for all thermal characteristics. However, the interaction between fermentation duration and extraction layer was significant (P<0.05) only for the onset temperature. Moreover, the three-way interaction for enthalpy was significantly (P<0.05) different (Table 3).

Table 3
Onset temperature, peak temperature, and enthalpy of starch Jir extracted from decorticated pearl millet grains as influenced by pearl millet genotypes, fermentation time, extraction layers, and their possible interactions.

	Thermal properties of the extracted starch (Jir)		
Genotypes	Onset temperature (°C)	Peak temperature (°C)	Enthalpy H (j/g)
Ashana	69.1 (±0.2)^{A}	73.8 (±0.2)^{A}	8.2 (±0.5)^{A}
Bioda	69.7 (±2.0)^{A}	73.8 (±1.8)^{A}	8.2 (±0.7)^{A}
Dembi-green	67.3 (±1.0)^{A}	72.5 (±1.0)^{A}	8.3 (±0.6)^{A}
Dembi-red	69.6 (±0.2)^{A}	74.2 (±0.2)^{A}	9.0 (±0.3)^{A}
Mayoa	69.3 (±0.1)^{A}	74.3 (±0.2)^{A}	8.3 (±0.5)^{A}
Fermentation periods			
1 Day	68.2 (±0.5)^{B}	73.1 (±0.6)^{A}	8.3 (±0.4)^{A}
7 days	69.8 (±0.7)^{A}	74.4 (±0.6)^{A}	8.5 (±0.3)^{A}
Extraction layers			
Lower	68.3 (±0.3)^{B}	73.0 (±0.4)^{B}	8.4 (±0.4)^{A}
Upper	69.7 (±0.8)^{A}	74.5 (±0.7)^{A}	8.4 (±0.2)^{A}
Three-Way ANOVA			
Genotypes, G	1.7^{NS}	1.1^{NS}	1.2 ^{NS}
Fermentation, F	5.4*	3.9^{NS}	0.4 ^{NS}
Layers, L	4.7*	5.9*	0.0 ^{NS}
G*F	4.0**	4.8**	7.6***
G*L	5.3**	6.5***	8.9***
F*L	5.3*	1.9^{NS}	0.2 ^{NS}
G*F*L	2.2^{NS}	1.0^{NS}	13.2***

For the effect sizes the regarding the onset temperature, the interaction between genotype and fermentation was the dominant contributor ($\eta^2 = 0.182$; Cohen's f = 0.702), with substantial contributions from genotype × layer ($\eta^2 = 0.160$; Cohen's f = 0.658) and genotype × fermentation × layer ($\eta^2 = 0.079$; Cohen's f = 0.462). Effects of individual factors such as genotype ($\eta^2 = 0.069$; Cohen's f = 0.432), fermentation ($\eta^2 = 0.057$; Cohen's f = 0.393), and layer ($\eta^2 = 0.037$; Cohen's f = 0.317) were comparatively minor (Table S3).

Regarding the peak temperature, genotype × layer was the dominant factor ($\eta^2 = 0.221$; Cohen's f = 0.761), followed closely by genotype × fermentation ($\eta^2 = 0.210$; Cohen's f = 0.742). A moderate contribution was observed for genotype × fermentation × layer ($\eta^2 = 0.039$; Cohen's f = 0.319) and layer alone ($\eta^2 = 0.051$; Cohen's f = 0.366). Other effects were relatively minor (Table S3).

Regarding the enthalpy, the three-way interaction between genotype, fermentation, and layer was the dominant contributor ($\eta^2 = 0.307$; Cohen's f = 1.112), with substantial effects from genotype × layer ($\eta^2 = 0.237$; Cohen's f = 0.978) and genotype × fermentation ($\eta^2 = 0.169$; Cohen's f = 0.824). Contributions from the individual factors were minor (Table S3).

The Data were evaluated using three-way ANOVA, and the factors were five pearl millet genotypes, fermentation time, and extraction layers. Means with identical superscript letters indicate that the values do not differ significantly at $p < 0.05$, according to Tukey's HSD. Asterisks (*) indicate significantly influential factors as ns, but they are insignificant. **significant at $p \leq 0.01$.*** significant at $p \leq 0.001$ level. Each value is the average of three replicates. Data in parentheses are the standard error of means.

3.4. Pasting properties

The pasting properties of the extracted pearl millet starch *Jir* were analyzed to identify variations across Sudanese pearl millet genotypes, fermentation durations, and starch extraction layers. The analysis revealed significant ($P<0.05$) differences in pasting properties, including peak viscosity, trough 1, breakdown, final viscosity, setback, peak time across pearl millet genotypes, fermentation duration, extraction layers, and their interactions (Table 4). A seven-day fermentation period resulted in significantly ($P<0.05$) higher values for pasting temperature, peak viscosity, Trough 1, final viscosity, setback, and peak time than the one-day fermentation period. However, the one-day fermented sample exhibited the highest breakdown rate. The extraction layers also played a crucial role in influencing pasting properties. The lower *Jir* layers showed significantly ($P<0.05$) higher peak viscosity, Trough 1, breakdown, final viscosity, setback, and peak temperature than the upper layers. An inverse relationship was observed for pasting temperature, where the upper layer exhibited the highest pasting temperature (Table 4). Among the pearl millet genotypes, Bioda exhibited the highest peak viscosity, Trough 1, breakdown, final viscosity, and setback compared to all other samples tested, except for pasting temperature. Mayoa had the highest pasting temperature and peak time, whereas *Jir* extracted from Ashana showed the lowest values for peak viscosity, Trough 1, breakdown, final viscosity, and setback. Additionally, Dembi-green had the shortest peak time (Table 4).

For the effect sizes the pasting properties of extracted Jir starch were significantly influenced by genotype, fermentation duration, and extraction layer, with varying effects across traits. Peak viscosity was mainly affected by genotype ($\eta^2 = 0.282$, $f = 34.27$), fermentation ($\eta^2 = 0.253$, $f = 32.46$), and layer ($\eta^2 = 0.179$, $f = 27.34$), with a notable genotype × layer interaction ($f = 15.47$) (Table S4).

Trough viscosity was primarily driven by fermentation ($\eta^2 = 0.530$, $f = 12.84$), with smaller effects from genotype and layer. Breakdown viscosity was mainly influenced by genotype ($\eta^2 = 0.336$, $f = 8.01$) and layer ($\eta^2 = 0.264$, $f = 7.10$), while fermentation had a negligible effect. Final viscosity was affected by genotype ($\eta^2 = 0.239$, $f = 11.14$), fermentation ($\eta^2 = 0.284$, $f = 12.14$), and layer ($\eta^2 = 0.078$, $f = 6.37$) (Table S4).

Setback viscosity was predominantly influenced by genotype ($\eta^2 = 0.280$, $f = 5.06$), with minor effects from layer and fermentation. Peak time was moderately affected by fermentation ($\eta^2 = 0.402$, $f = 2.66$) and genotype ($\eta^2 = 0.191$, $f = 1.84$). Pasting temperature showed moderate effects from fermentation ($\eta^2 = 0.288$, $f = 4.09$), genotype ($\eta^2 = 0.186$, $f = 3.29$), and layer ($\eta^2 = 0.173$, $f = 3.17$) (Table S4).

3.4.1. Texture profiles

Regarding the pearl millet genotypes, Dembi-red exhibited significantly ($P<0.05$) higher hardness levels than the other tested genotypes. The Bioda and Dembi-green genotypes had similar hardness levels, which were significantly ($P<0.05$) higher than that of Mayoa, which had the lowest hardness. Mayoa also had the lowest cohesiveness, which was

Table 4
Pasting properties of jir starch extracted from dehulled grains of sudanese pearl millet genotypes in response to fermentation duration and extraction layer, including pasting temperature, peak viscosity, trough 1, breakdown, final viscosity, setback, and peak time.

	Pasting properties of extracted pearl millet starch (Jir)						
Genotypes	Pasting Temp (°C)	Peak viscosity (cP)	Trough 1 (RVU)	Breakdown (cP)	Final Viscosity (RVU)	Setback (cP)	Peak Time (min)
Ashana	87.7 (±0.7)^{D}	1600.1 (±96.3)^{D}	1101.6 (±63.0)^{C}	498.5 (±45.1)^{C}	2004.1 (±129.5)^{D}	902.5 (±68.2)D	5.60 (±0.04)^{B}
Bioda	88.6 (±0.4)^{B}	1941.1 (±93.9)^{A}	1257.6 (±74.8)^{A}	683.5 (±29.6)^{A}	2345.5 (±100.5)^{A}	1087.9 (±30.5)A	5.67 (±0.02)^{A}
Dembi-green	88.0 (±0.2)^{C}	1555.1 (±87.9)^{E}	1017.5 (±57.7)^{D}	537.6 (±32.0)^{E}	1848.3 (±93.8)^{E}	830.8 (±39.7)E	5.55 (±0.03)^{C}
Dembi-red	87.2 (±0.5)^{E}	1802.4 (±32.7)^{B}	1126.0 (±32.0)^{B}	676.4 (±22.4)^{B}	2126.9 (±32.4)^{B}	1000.9 (±32.4)B	5.59 (±0.03)^{B}
Mayoa	89.4 (±0.3)^{A}	1630.4 (±42.2)^{C}	1106.5 (±24.7)^{C}	523.9 (±96.3)^{C}	2072.3 (±39.9)^{C}	965.8 (±30.6)C	5.68 (±0.03)^{A}
Fermentation periods							
1 Day	87.3 (±0.3)^{B}	1571.8 (±52.6)^{B}	980.9 (±25.1)^{B}	590.9 (±32.5)^{A}	1906.0 (±39.9)^{B}	925.1 (±35.7)B	5.55 (±0.02)^{B}
7 days	89.1 (±0.2)^{A}	1839.9 (±32.3)^{A}	1262.9 (±24.8)^{A}	577.1 (±14.6)^{B}	2252.9 (±39.9)^{A}	990.0 (±23.8)A	5.67 (±0.01)^{A}
Extraction layers							
Lower	87.5 (±0.3)^{B}	1822.7 (±35.3)^{A}	1169.0 (±33.7)^{A}	653.7 (±14.8)^{A}	2176.9 (±39.9)^{A}	1007.9 (±19.8)A	5.63 (±0.02)^{A}
Upper	88.9 (±0.2)^{A}	1589.0 (±53.9)^{B}	1074.7 (±36.5)^{B}	514.3 (±26.8)^{B}	1982.0 (±39.9)^{B}	907.3 (±36.7)B	5.61 (±0.04)^{B}
Three-Way ANOVA							
Genotypes, G	120.8***	11853.8***	489.0***	659.6***	1209.5***	245.3***	34.9***
Fermentation, F	654.5***	40874.1***	6484.7***	20.1***	5504.6***	135.8***	277.4***
Layer, L	383.9***	31059.6***	725.1***	2035.4***	1737.6***	326.3***	8.5**
G*F	42.5***	1830.4***	272.1***	286.8***	888.3***	249.2***	17.8***
G*L	57.2***	2362.7***	173.0***	144.9***	526.6***	149.7***	19.6***
F*L	34.2***	2472.4***	9.2**	320.7***	188.5***	92.6***	18.1***
G*F*L	70.2***	7147.4***	345.0***	235.7***	570.4***	101.1***	15.4***

The Data were evaluated using a three-way ANOVA, and the factors were five pearl millet genotypes, fermentation time, and extraction layers. According to Tukey's HSD, means with identical superscript letters do not differ significantly at $p < 0.05$. Asterisks (*) indicate significantly influential factors as ns, but they are insignificant. **significant at $p \leq 0.01$.***significant at $p \leq 0.001$ level. Each value is the average of 3 replications. Data in parentheses are the standard error of means.

significantly (P<0.05) lower than that of other genotypes. The Bioda, Dembi-green, and Dembi-red genotypes exhibited similar springiness levels, which were considerably higher than those of Ashana and Mayoa. Bioda had the highest adhesiveness, which was significantly (P<0.05) higher than that of the other tested genotypes (Table 5).

For the effect sizes the extraction layers were the most influential factor affecting all gel textural parameters, with large effect sizes for hardness ($\eta^2 = 0.377$, $f = 9.749$) and adhesiveness ($\eta^2 = 0.247$, $f = 1.783$). Pearl millet genotypes moderately affected hardness ($\eta^2 = 0.148$, $f = 6.109$) and adhesiveness ($\eta^2 = 0.109$, $f = 1.187$). In contrast, fermentation periods had the most significant impact on cohesiveness ($\eta^2 = 0.173$, $f = 1.437$) and moderate effects on springiness ($\eta^2 = 0.186$, $f = 1.403$) and adhesiveness ($\eta^2 = 0.111$, $f = 1.195$). Significant interaction effects were observed for genotypes × fermentation periods × extraction layers, particularly in hardness ($f = 9.137$), cohesiveness ($f = 1.635$), springiness ($f = 1.345$), and adhesiveness ($f = 1.410$), indicating combined influences of genotypes and processing factors (fermentation periods, extraction layers) on starch gel texture (Table S5).

The Data were evaluated using a three-way ANOVA, and the factors were five pearl millet genotypes, fermentation time, and extraction layers. According to Tukey's HSD, means with identical superscript letters do not differ significantly at $p < 0.05$. Asterisks (*) indicate significantly influential factors as ns, but they are insignificant. **significant at $p \leq 0.01$.***significant at $p \leq 0.001$ level. Each value is the average of 3 replications. Data in parentheses are the standard error of means

Fig. 3, Fig. 4, Fig. 5

3.5. PCA and PLS

The first principal component (PC1) explained nearly 34 % of the total variation, primarily differentiating the samples based on color measurements, gel texture profiles, and pasting properties (Fig. 6a). Physicochemical and thermal properties primarily contributed to the second principal component (PC2), accounting for approximately 21.8 % of the total variation. *Jir* samples from the lower layer generally had positive PC1 values, indicating higher whiteness index (WI), lower a*, b*, and ΔE values, and higher pasting properties compared to samples from the upper layer (Fig.s 6a and 6b). The PCA score plot (Fig. 6b) scattered *Jir* samples from different genotypes and fermentation times, indicating a lack of a coherent pattern in starch quality variation based on genotype or fermentation alone.

The *Jir* samples were separated using partial least squares regression analysis (PLS). The first PLS component had positive values for the samples in the lower layer and negative values for the upper layers (Fig. 7a). No clear relationship was observed between genotype, fermentation time, and PLS component values. The highest positive value for the first PLS component was observed in the lower-layer sample of the Bioda genotype fermented for 7 days (Fig. 7a).

The PLS model with one component yielded a cumulative Q^2 value of 0.260, R^2Y of 0.397, and R^2X of 0.397. With two components, model quality improved, reaching a cumulative Q^2 of 0.396, R^2Y of 0.590, and R^2X of 0.590 (Supplementary 6). The PLS loading plot analysis identified color measurements (WI, b*, and ΔE) and pasting properties (final viscosity and hardness) as key variables explaining the variance in the first PLS component (Fig. 7b). The PLS component values for these variables were -0.311 for WI, 0.310 for b*, 0.301 ΔE, -261 for final viscosity, and -0.259 for hardness. Additionally, high values for the first PLS component were obtained for the peak viscosity (-0.309), trough 1 (-0.269), and adhesiveness (-0.271) (Fig. 2b). The variables were identified as the most important contributors to sample variation according to their variable importance in projection (VIP). Specifically, WI and b* had VIP values of 14 and 148, respectively (Fig. 7c) with minimal standard errors. The VIP values for peak viscosity (14.8) and ΔE (14.4) were also significant, whereas adhesiveness and trough 1 had VIP values of 12.9 and 12.8, respectively (Fig. 7c). Some variables, such as the final viscosity, hardness, and breakdown, had moderate effects, whereas the onset temperature had the least negligible impact.

Table 5
Textural Profile of Starch Extracted from Dehulled Grains of Five Sudanese Pearl Millet Genotypes in Response to Fermentation Duration and Extraction Layer, Including Hardness, Cohesiveness, Springiness, and Adhesiveness.

Genotypes	Texture profiles of extracted pearl millet starch (*Jir*)			
	Hardness (g)	Cohesiveness	Springiness (mm)	Adhesiveness (mJ)
Ashana	70.9 (±5.1)^{C}	0.47 (±0.02)^{A}	10.0 (±0.1)^{B}	0.38 (±0.05)^{B}
Bioda	79.1 (±5.9)^{B}	0.48 (±0.01)^{A}	10.7 (±0.4)^{A}	0.53 (±0.08)^{A}
Dembi-green	77.1 (±4.3)^{B}	0.48 (±0.01)^{A}	10.4 (±0.3)^{AB}	0.35 (±0.06)^{B}
Dembi-red	90.1 (±4.5)^{A}	0.47 (±0.01)^{A}	10.6 (±0.3)^{A}	0.35 (±0.03)^{B}
Mayoa	57.8 (±4.3)^{D}	0.45 (±0.01)^{B}	10.0 (±0.1)^{B}	0.43 (±0.04)^{B}
Fermentation periods				
1 Day	72.5 (±4.6)^{B}	0.48 (±0.01)^{A}	10.8 (±0.2)^{A}	0.34 (±0.03)^{B}
7 days	77.6 (±5.5)^{A}	0.45 (±0.01)^{B}	10.0 (±0.1)^{B}	0.47 (±0.04)^{A}
Extraction layers				
Lower	92.0 (±3.6)^{A}	0.48 (±0.01)^{A}	10.1 (±0.1)^{B}	0.51 (±0.04)^{A}
Upper	58.0 (±4.5)^{B}	0.46 (±0.01)^{B}	10.7 (±0.2)^{A}	0.30 (±0.03)^{B}
Three-Way ANOVA				
Genotypes, G	372.4***	10.0***	11.0***	13.1***
Fermentation, F	85.7***	87.1***	75.3***	50.7***
Layer, L	3811.0***	24.8***	45.1***	132.3***
G*F	157.8***	19.2***	13.3***	16.2***
G*L	164.5***	27.4***	7.9***	20.6***
F*L	14.5***	0.9°	60.9***	7.5***
G*F*L	828.3***	26.6***	18.2***	19.5***

3.6. Correlation between measurements

The correlation between the measurements in this study is shown in Fig. 8. Significant negative correlations were observed between amylose content and pasting temperature (R= -0.68; P<0.05) and between amylose content and Trough1 viscosity (R= -0.55; P<0.05). Similarly, amylose content was negatively correlated with the peak time (R=-0.48; P<0.05). In contrast, amylose content was positively correlated with cohesiveness (R=0.48; P<0.05).

Regarding water adsorption capacity (WAC), significant positive correlations were found between WAC and peak viscosity (R=0.48; P<0.05) as well as between WAC and peak viscosity Trough 1 viscosity (R=0.48; P<0.05). For the gel textural profiles, both adhesiveness (R=0.56; P<0.05) and hardness (R=0.50; P<0.05) were positively correlated with WAC. Starch damage showed positive correlations with peak viscosity (R=0.48; P<0.05) and Trough1 (R=0.47; P<0.05). A similar trend was observed between starch damage and adhesion (R=0.56; P<0.05) and between starch damage and hardness (R=0.50; P<0.05).

4. Discussion

The physicochemical properties of the extracted *Jir,* such as amylose content, bulk density, water absorption capacity, and starch damage content, varied significantly based on pearl millet genotypes, fermentation times, extraction layers, and possible interactions. Notably, the bulk density, water absorption capacity, and starch damage increased after seven days of fermentation compared to just one. Increasing the

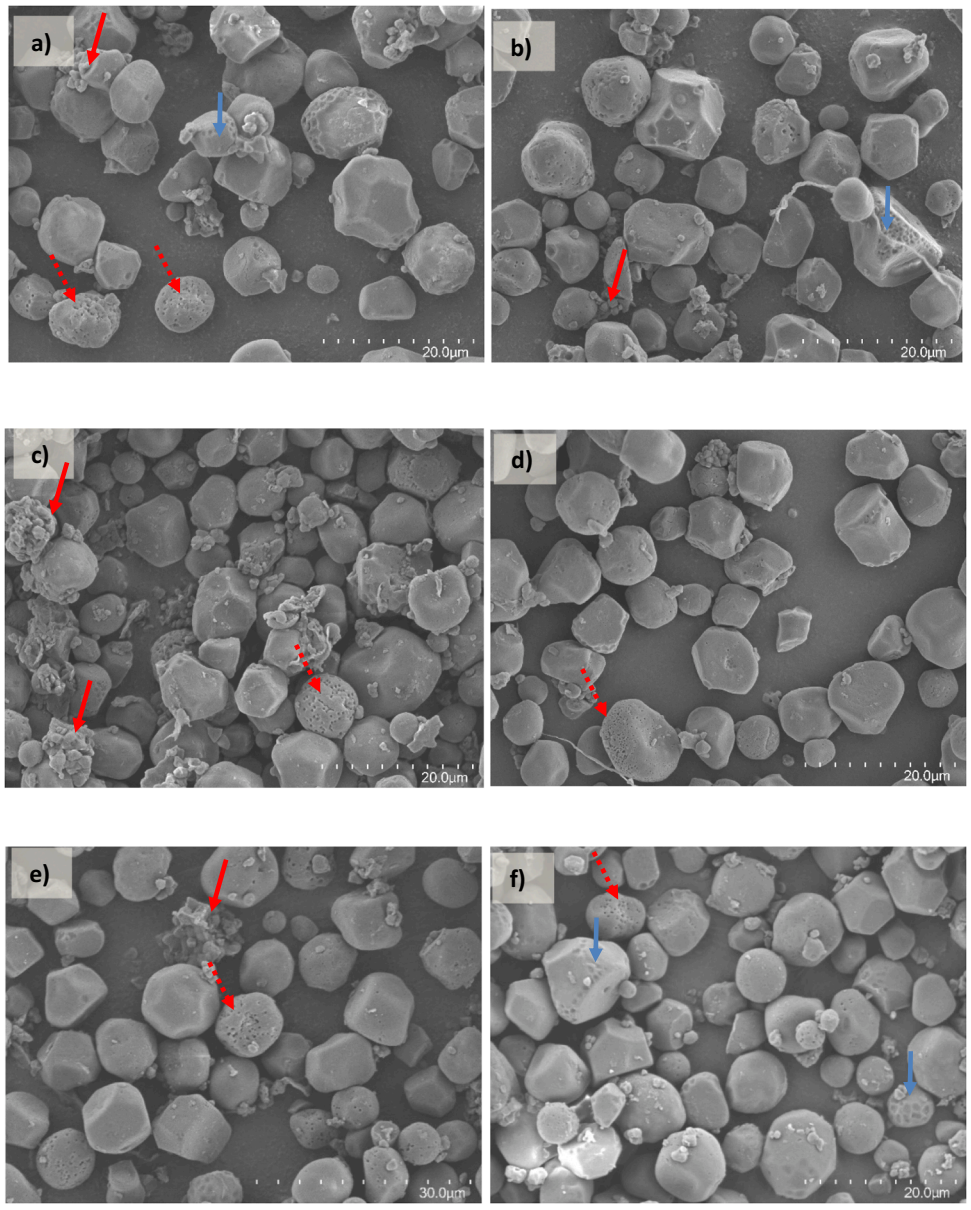

Fig. 3. SEM micrographs of upper (U) and lower (L) layers of fermented starch *(Jir)* after 7 days, a) Ashana L, b) Ashana U, c) Bioda U, d) Dembi-green L, e) Dembi-red U, and f) Mayoa L. Dotted red arrows show porous granules, white arrows show indentations, and solid red arrows show broken starch and non-starch components.

bulk density of *Jir* by fermenting it for seven days is similar to a fermented starchy product (Gari) made from cassava tubers (Owuamanam et al., 2010) In their study, bulk density increased after two days of fermentation. It remained stable until day six, with an additional increase by day eight. The consistency across different starchy ferments, as seen in Jir's works, supports the notion that fermentation affects bulk density similarly to other starch-based foods. The structural modification of the starch granule morphology during fermentation, which may lead to enhanced packing density and water-holding capacity, might also be responsible for increased bulk density.

The study further demonstrated that longer fermentation time (7 days) significantly increased the water-absorbing capacity and starch damage in *Jir*. The longer fermentation time contributed to changes in starch granule morphology, including pores, indentations, and granule degradation. In our previous study, changes in starch granule morphology also contribute to an increase in hydrolysis rate and in-vitro digestibility (Hamid et al., 2025). When these starch granules are subjected to wet conditions, they can trigger the breakdown of crystalline regions, which might lead to high water absorption. This reduction in the crystalline regions and the emergence of amorphous areas in *Jir* likely allow more water to interact, thereby enhancing the water absorption capacity (Bankole et al., 2013).

Moreover, longer fermentation time resulted in a marked increase in starch damage, likely due to the action of enzymes such as amylases released by microorganisms during fermentation. This enzymatic breakdown of *Jir* starch granules can lead to textural changes and impact starch's physicochemical properties, potentially affecting the shelf life and quality of the final product (Kumar et al., 2021; Mohamed et al., 2019).

Conversely, the amylose concentration of *Jir* decreased significantly during the 7-day fermentation period. This outcome aligns with Osungbaro (1990), who reported a progressive reduction in amylose content up to 20 %) in fermented maize porridge "*Ogi*" during the first two days of fermentation, followed by another six days of souring. Similarly, Adeyemi and Beckley (1986) attributed this reduction to the activity of amylolytic microorganisms, which degrade amylose into

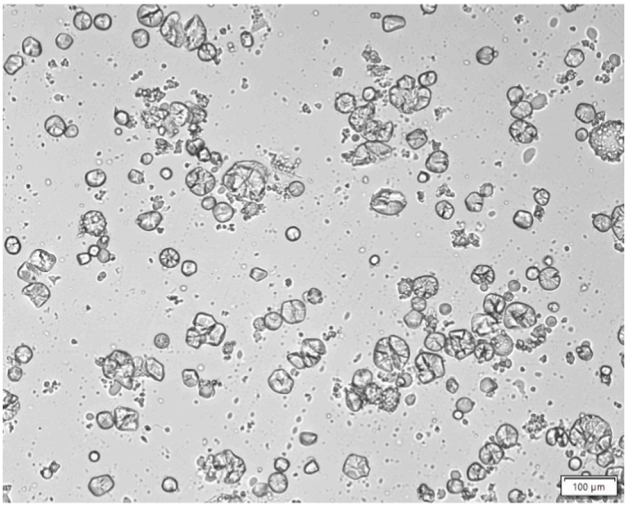

Fig. 4. Light microscopy image of *Jir hur* starch granules from the Dembi-red variety (7-day fermented), showing a visual change in granule morphology under wet conditions.

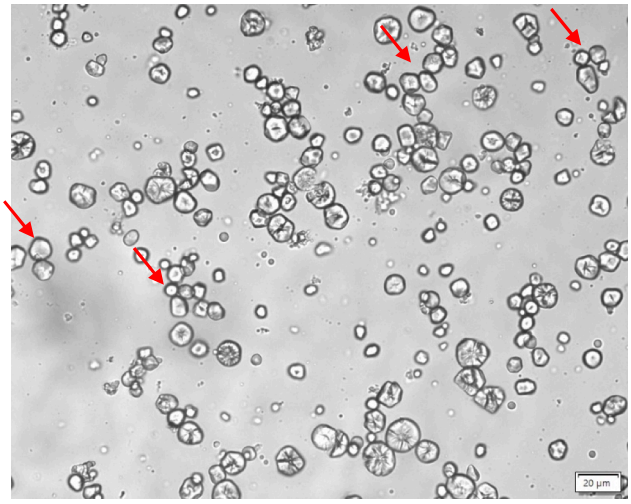

Fig. 5. Light microscopy image of *Jir hur* starch granules from Ashana (7-days fermented). Red arrows show smaller intact starch granules in wet conditions.

simpler sugars during fermentation. However, contrary findings by Purewal et al. (2024) demonstrated that solid-state fermentation significantly increased amylose content. The reduction of amylose content in *Jir* during fermentation likely influences its functional properties, including bulk density, texture, and water-holding capacity.

Our findings revealed significant variations in amylose content, bulk density, water absorption capacity, and starch damage in *Jir* extracted from different Sudanese pearl millet genotypes. For instance, Ashana, with its high amylose content, is well-suited for firm gels or products aimed at glycemic control. Mayoa, owing to its high bulk density and low starch damage, is ideal for products that require a dense texture and slow digestion. In contrast, Bioda and Dembi-red, with their high water absorbance capacities, are optimal for moisture-retentive applications. Starch damage varied among the genotypes, with Bioda exhibiting the highest level (3.20 %) and Mayoa the lowest (3.0 %). High levels of damaged starch can benefit products that require rapid starch gelatinization; however, this may lead to undesirable textural changes during storage. In contrast, Mayoa's lower starch damage suggests a more intact granule structure, making it preferable for products that require slow digestion or stable texture over time.

Our findings indicate that the lower layer, *Jir Hur,* has higher amylose content, bulk density, water absorption capacity, and starch damage than the upper layer, *Khadim*. This result was attributed to the smaller granule size and relatively less surface damage in *Jir Hur*, which prevented water and enzymes from penetrating them during the fermentation. A correlation to smaller granule size and higher amylose content has been reported in cereal and legume starches (Kaur et al., 2010; Sandhu et al., 2004; Sandhu & Siroha, 2017). The granules in the upper layer contained relatively larger-sized granules and showed morphological changes to the granule surface (pores, indentations, and granule breakdown) after fermentation. This allows better enzyme penetration, leading to amylose breakdown (Hamid et al., 2025). Previous studies on the spontaneous fermentation of pearl millet have also shown a decrease in amylose content after a 24 h fermentation period (Gupta & Gaur, 2024a). Another study on the spontaneous fermentation of glutinous proso millet has shown a gradual increase in amylose content after 48h and then a gradual decrease after 96 h (Bian et al., 2022). The initial increase in amylose content was attributed to the breakdown of amylopectin side chains, which resulted in the production of smaller, detached amorphous molecules that contributed to the observed increase in amylose. However, with extended fermentation time, enzymatic and acid hydrolysis eventually break down the amylose-rich regions. These findings are consistent with the results observed in this study.

The higher bulk density observed in this study can be explained by the fact that the fraction with a density lower than that of the gelatinized granules corresponds to lower-density starch granules that are closely packed, thus reducing the interstitial space between the granules (Abebe et al., 2015).

The pearl millet cultivar, fermentation time, and extraction layer significantly affected colorimetric parameters L^*, a^*, b^*, ΔE, and WI (Table 2). A fermentation period of 7 days was found to increase the brightness (L*) and whitening index (WI) while decreasing the a^*, b^*, and ΔE of the *Jir* samples compared to a fermentation period of 1 day. Similar results were reported by Gong et al. (2020). The L* values and WI increased with prolonged fermentation time for gelatinized potato flour. In contrast, the a* (redness), b^* (yellowness), and ΔE values (total color difference) decreased. In a recent study, Im et al. (2023) demonstrated that the natural fermentation of mushroom mycelia enhanced WI, highlighting the potential of fermentation processes in various applications. These authors suggested that increased whiteness and brightness with extended fermentation might result from yeast fermentation purifying the flour and breaking down carotenoid pigments. Microorganisms degrade lipids and carbohydrates into alcohols and organic acids, preventing pigment degradation. The observed change in *Jir* color is likely due to gelatinization caused by temperature and pressure during natural fermentation. This suggests that extended fermentation may lead to a more refined starch appearance with less color saturation and a higher degree of whiteness.

Compared to the other genotypes, Dembi-red exhibited higher L^* and WI values, indicating that it produces starch with better whiteness and overall appearance. In addition, the Bioda genotype had the highest a^* value, suggesting that its pulp was red. By contrast, Dembi-green had the highest b^* value, implying it was more yellow than the other samples. These differences in color between pearl millet genotypes reflect genetic variation in the crop. Therefore, specific genotypes may be more appropriate for industrial applications based on the color characteristics. The lower ΔE value in the Mayoa genotype suggests that it underwent minimal color change during processing, which could be beneficial for maintaining product quality. However, the increase in WI in Dembi-red indicates that it can produce starch with a darker color, which may be advantageous for companies processing products for the food and non-food industries.

Our results showed that *Jir* extracted from all pearl millet genotypes exhibited similar thermal properties. This lack of genotypic variation contrasts with the findings of Chávez-Murillo et al. (2011) on Mexican

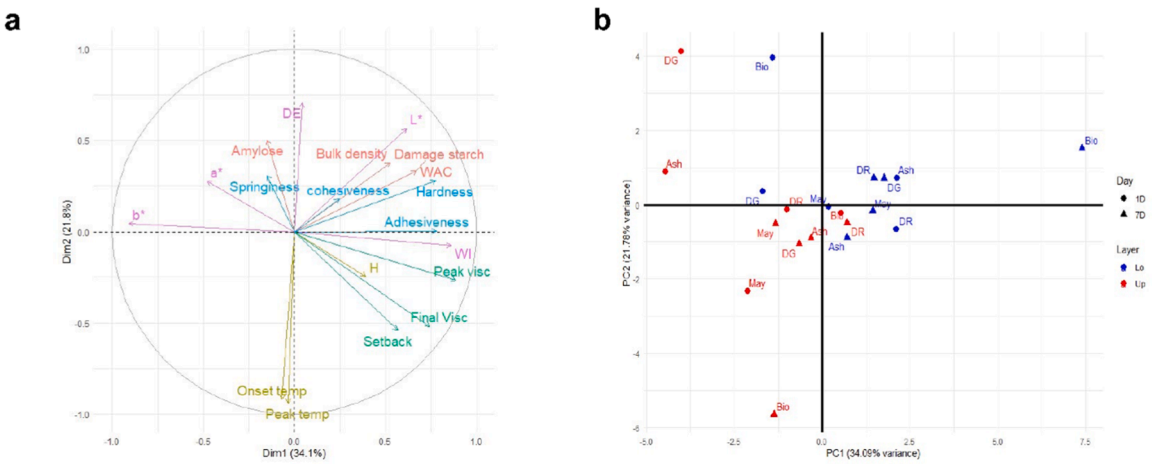

Fig. 6. Loading (A) and score (B) plots from principal component analysis of starch quality parameters in starch "jir" samples from different genotypes (Ash = Ashana, Bio = Bioda, DG = Dembi-green, DR = Dembi-red, May = Mayoa), fermentation times (1 day = 1D, 7 days = 7D), and layers (lower, upper). In the loading plot, physicochemical characteristics of the starch (amylose= amylose content, damaged starch, WAC = water absorption capacity, bulk density) are marked in orange text. Color measurements (lightness, a* = redness/greenness, b* = yellowness/blueness, WI = whiteness index, DE = total color difference) are marked in purple text. Thermal properties (onset temp = onset temperature, peak temp = peak temperature, H = enthalpy) are shown in light green text. Pasting properties (setback, final viscosity, and peak viscosity) are labeled in dark green, while textural properties (hardness, cohesiveness, springiness, adhesiveness) are in blue. In the score plot, ● =1day fermentation, and Δ =7-day fermentation. Blue symbols represent lower-layer samples, and red symbols represent upper-layer samples.

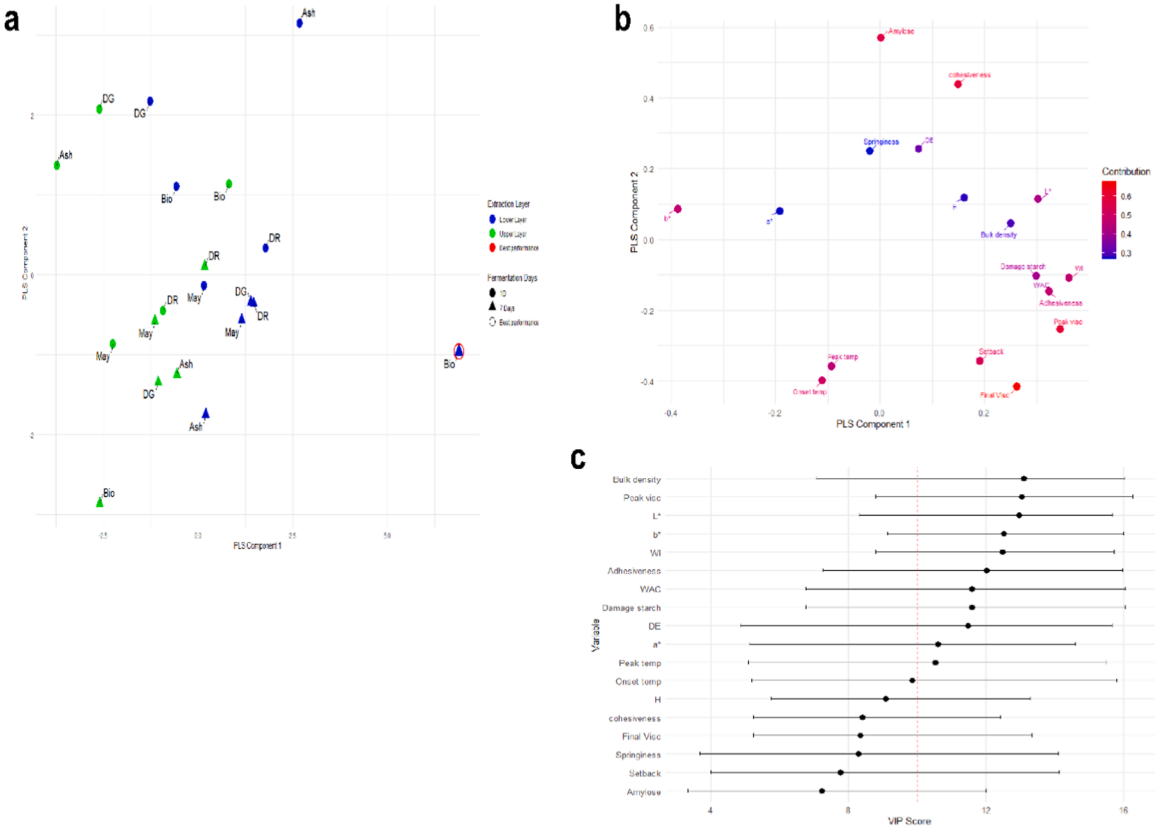

Fig. 7. (a) Partial Least Squares regression analysis (PLS) for the physiochemical, colorimetric, thermal, pasting, and gel texture properties of starch Jir extracted from five Sudanese pearl millet genotypes in response to fermentation time and extraction layer. (b) Line loading plot of active variable for the first two components in the PLS model. (c) Variable importance for the projection (VIP) scores and 95 % confidence interval (bootstrap method) of the active variable for the first two components in the PLS model. The red borderlines were plotted to mark the physiochemical, colorimetric, thermal, pasting, and gel texture properties of Jir with VIPs over 10.

rice genotypes and Kim et al. (2007) on mung bean starches, which emphasize the importance of cultivar-specific differences in the thermal properties of starch. Similarly, Agama-Acevedo et al. (2014) found that cooked banana starch had higher gelatinization temperatures and enthalpies than desert banana genotypes. One possible explanation for the lack of genotypic variation in our study could be the influence of the fermentation process, which may have reduced the impact of genotype on the thermal properties of *Jir* starch. The fermentation process can

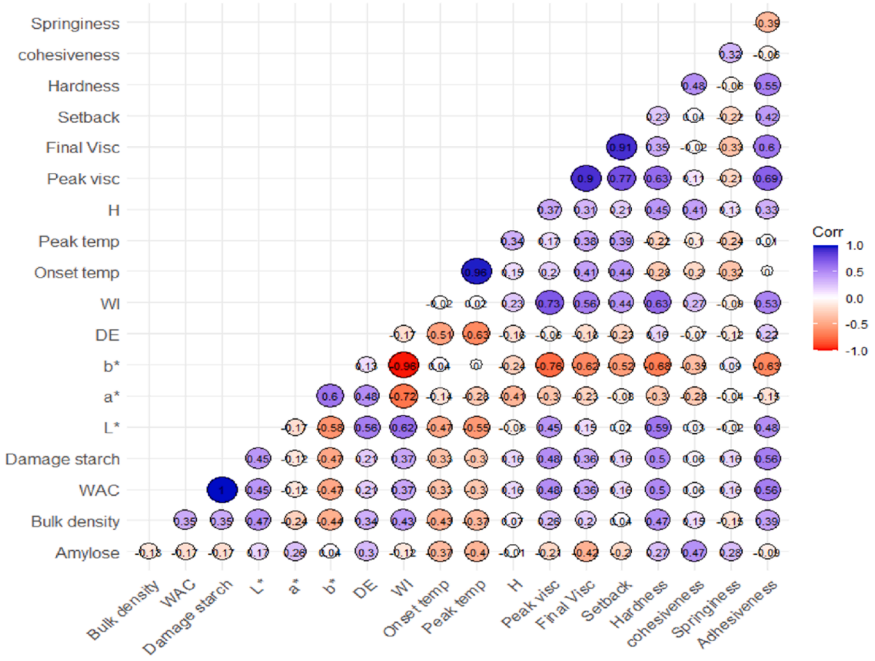

Fig. 8. Correlation plot of relationships between the measurements.

lead to significant structural changes in starch, potentially masking any inherent genotypic differences. Moreover, the fermentation duration may play a more prominent role in determining the thermal properties, as Wu et al. (2022) observed that the gelatinization onset temperature increases with longer fermentation durations, while gelatinization enthalpy decreases. Wu, who reported that the onset temperature of gelatinization rises with fermentation duration, while the gelatinization enthalpy decreases.

Similarly, several reports have demonstrated that natural fermentation results in significant changes in the gelatinization behavior of starch, including the onset temperature, peak temperature, conclusion temperature, and enthalpy (Gupta & Gaur, 2024b; Hong et al., 2022; Ilowefah et al., 2015). This study did not reveal any changes in peak temperature or enthalpy with fermentation duration. This suggests that while genotype-specific differences might be present under non-fermented conditions, the fermentation process could be a dominant factor influencing the thermal properties of *Jir* starch in our study.

The pasting properties *Jir* from different Sudanese pearl millet genotypes depend on the fermentation period, extraction layers, and possible interactions. The pasting profile, including pasting temperature, peak viscosity, trough 1, final viscosity, setback, and peak time, was enhanced after seven days of fermentation compared to the initial fermentation. Li et al. (2019) attributed the increase in peak viscosity during prolonged fermentation to the rise in short-chain amylopectin and amylose, which enhances water absorption capacity and facilitates starch granules swelling, significantly increasing peak viscosity. In addition, the higher peak viscosity is linked to the proliferation of proteolytic bacteria, which degrade protein structures and release starch granules. In contrast, the breakdown viscosity decreased with increasing fermentation duration of up to seven days. These findings support the recent report by Chauhan et al. (2024), who reported a significant reduction in the breakdown viscosity of starch isolated from foxtail and barnyard millets after seven days of fermentation. Likewise, Chandrasekar et al. (2022) observed a higher breakdown in finger millet starch after four days of solid-phase fermentation with *Aspergillus oryzae*. The reduction in the breakdown viscosity of millet starch can be attributed to the disintegration of the gelatinized starch granules. These findings suggest that extended fermentation improves the rheology of starch dispersions, enhances enzyme activity, and induces various biochemical changes (Aloys & Zhou, 2006; Dang & Copeland, 2004; Obadina et al., 2013).

This investigation revealed that the measured pasting properties of *Jir*, including peak viscosity, trough 1, breakdown, final viscosity, setback, and peak temperature, were significantly higher in the lower *Jir* layer compared to the upper layer. These differences may be attributed to the higher concentrations of starch and other macromolecules in the lower *Jir* layer, which influence viscosity and paste stability. In contrast, the higher pasting temperature of the upper layer (*Khadim*) can be explained by variations in thermal properties, granule size, amylose content, and the presence of non-starch polysaccharides.

The pasting properties of the pearl millet genotypes showed considerable variation. Bioda exhibited the highest peak viscosity, Trough1, breakdown, final viscosity, and setback. Mayoa had the best pasting temperature and peak time among the pearl millet genotypes, indicating that its gelatinization requires more thermal energy. The lowest viscosity was observed in the *Jir* isolated from Ashana, which had the lowest density and was less stable as a starch paste. Dembi-Green demonstrated rapid pasting behavior, characterized by quick hydration and gelatinization. Variations in the adhesive properties of different genotypes highlight the importance of selecting appropriate genotypes for specific applications. For instance, the high viscosity and stability of Bioda make it ideal for products exposed to heat. At the same time, the fast-pasting characteristics of Dembi-Green could be beneficial for ready-to-eat food production.

This study demonstrated significant variations in the gel texture profiles, including hardness, cohesiveness, springiness, and adhesiveness, of *Jir* samples from the five pearl millet genotypes, fermentation times, and extraction layers. The significant hardness, cohesiveness, springiness, and adhesiveness differences among the five Sudanese pearl millet genotypes suggest a strong genetic influence on these textural properties. For example, Dembi-red exhibited a higher starch *Jir* hardness than the other genotypes, which can be attributed to molecular differences, such as the content of specific starch molecules and granules. The gel formed by Dembi-red also had a higher density than the other samples. While Dembi-red may be slightly harder, this increased hardness could benefit products that require a firmer texture. In contrast, Mayoa produced a less cohesive gel, making it less suitable for applications that require a firm foundation and stability.

One-day fermentation resulted in significantly higher gel cohesiveness but lower springiness than seven-day fermentation. Therefore, prolonged fermentation may increase gel tightness and stickiness, which is desirable for products that require enhanced structural cohesiveness. The results also showed that the *Jir* obtained from the lower *Jir* layer had higher hardness, cohesiveness, and adhesiveness than the *Jir* obtained from the upper layer. This suggests that millet grains contain two types of starches with distinct functional properties. Additionally, the higher springness of the upper layer indicates that its gel is more elastic, making it in applications where materials need to regain their shape after deformation.

The negative relationship between amylose content and pasting temperature, Trough 1 viscosity, and peak time indicates that *Jir* with higher amylose content exhibits lower pasting temperatures during the gelatinization of starchy materials. This may be because amylose is a linear polymer, which reduces the swelling capacity of the starch granules. As a result, the pasting temperature and viscosity are lower because the granules do not swell to the full swelling potential. The changes in the peak-time growth regression equation with increasing amylose content can be explained as follows: higher amylose starch content may increase peak viscosity during the earlier stages of heating, which can be useful in applications where rapid thickening at high temperatures is desired. Notably, cohesiveness increased with higher amylose content, suggesting that increased amylose improves the cohesive gel structure. This may be due to the amylose macromolecules present during cooling, which enhance the compatibility of the starch *Jir* gel. This property is fundamental in gel-containing *Jir* products, where a stable structure is needed, such as in desserts and processed foods.

The high positive coefficients between WAC and peak and Trough 1 viscosities indicated that *Jir* samples displayed higher viscosities during gelatinization due to their high WAC. This can be attributed to the relationship between amylose content and pasting viscosity, where amylose-rich starches swell more upon contact with water, thereby increasing viscosity. Furthermore, the positive correlation between WAC, adhesiveness, and hardness suggests that *Jir* with higher WAC content produces gels with strong adhesion and a firmer texture. This property is particularly beneficial in gel-based applications, such as confections and baking, where hardness is essential

The PCA results emphasized the importance of the extraction layer in determining the WI and pasting properties of *Jir* starch. The lower extraction layer, which exhibited a high WI of 95.4, was purer and more suitable for applications. According to Giuberti et al. (2019), the WI is a crucial parameter in evaluating the quality of extracted starch of white sorghum, as it reflects the degree of purity and the presence of impurities. This is especially important in industries where visual appeal is critical, such as producing transparent films and various food products. However, improving *Jir* starch quality requires a more integrated understanding of the interactions among pearl millet genotypes, fermentation conditions, and extraction processes. These factors must be carefully considered to optimize the properties of *Jir* starch to enable tailored applications and enhanced functionality.

The low-layer *Jir* samples of the Bioda genotype fermented for seven days had the highest positive score for the first PLS component. Differences in the structure and composition of the lower layer may be attributed to factors such as enhanced microbial or enzymatic degradation, variations in the distribution of amylose and amylopectin, and fewer impurities on *Jir* starch components. This could be attributed to the longer fermentation time, which might have enhanced the breakdown of undesirable compounds or altered the structural configuration of the starch, thereby improving the pasting properties and color values. This information is essential for determining the best processing techniques to enhance the functional properties of *Jir* starch based on the extraction and fermentation layers.

Our results revealed positive correlations between starch damage and the peak and trough 1 viscosities. Starch damage increased starch viscosity during gelatinization. Starch granules that are damaged swell at a higher rate, which accounts for their high viscosity. In addition, the results confirm that an increase in the extent of starch damage leads to firm gel adhesion formation. This may be reinforced by the observation that damaged starch granules contain more amylose upon gelatinization and interact to form a firm gel network. Although starch damage is beneficial, it should be closely controlled to overcome damage that can lead to undesirable textural properties.

Compared to commercially available starches such as corn and cassava, *Jir* showed distinctive functional properties, particularly viscosity and gelatinization. Commercial starches like corn starch are known for their high viscosity and consistent gelatinization behavior and are often used in thickening applications. In contrast, Jir's viscosity and gelatinization properties vary depending on genotype and fermentation duration, which can offer flexibility for diverse food applications. For example, while cassava starch shows relatively higher viscosity and stability in gel formation (Owuamanam et al., 2010), Jir's variable pasting properties may provide specific advantages in foods requiring customized textural characteristics. Furthermore, the water absorption capacity and starch damage of Jir, enhanced by fermentation, could offer functional benefits in applications requiring moisture retention or enhanced digestibility. Comparing these properties with those of corn and cassava starches highlights Jir's potential and its competitive advantages or limitations in various food formulations.

The high viscosity, setback, and final viscosity values observed, especially in the lower- and seven-day fermented samples, suggest that Jir starch can serve as an effective thickening and structuring agent, addressing common issues in gluten-free baking such as crumbliness and poor dough elasticity. Furthermore, its springiness, cohesiveness, and adhesiveness make it a promising alternative to synthetic binders or hydrocolloids in gluten-free formulations, such as breads, cakes, and pastries. In addition, the high gelatinization temperature of Jir indicates its thermal stability, which supports its application in products requiring heat resistance, such as gluten-free pasta, noodles, and baking mixes. Importantly, Jir starch offers a clean-label, indigenous, and nutrient-rich alternative to conventional starches, aligning with consumer trends favoring natural and culturally rooted ingredients.

5. Conclusions

Using the extraction layer, fermentation duration, and pearl millet genotype as input variables, this study demonstrated the potential to tailor the functional properties of *jir*, a traditional starch product derived from fermented pearl millet. Among the tested factors, the extraction layer emerged as the most influential, particularly affecting the colorimetric and pasting properties of Jir starch. Partial least squares (PLS) regression further highlighted that samples extracted from the lower layer of the Bioda genotype fermented for seven days exhibited the most desirable properties for preparing traditional porridges.

While the traditional method of Jir extraction remains culturally rooted and effective on a small scale, its scalability for industrial use poses several challenges, particularly in achieving consistent layer separation, optimizing fermentation time, and reducing labor intensity. Future work should explore automated extraction, optimized fermentation protocols, and improved separation technologies to enhance the production efficiency and feasibility for large-scale applications.

Moreover, we acknowledge that microbial activity likely plays a critical role in driving the biochemical modifications of starch during fermentation. Although meta-transcriptomic, metabolomic, and enzymatic analyses could elucidate the microbial dynamics and underlying mechanisms, such advanced techniques were beyond the scope of this study owing to budgetary and logistical constraints. These approaches and controlled bioreactor systems are proposed as essential directions for future investigations to improve the reproducibility, mechanistic understanding, and process control.

Ethical Statement

This study does not involve any human participants or animals. All experiments were conducted solely on plant-based materials, specifically pearl millet starch, and did not require any ethical approval for human or animal testing. The research adheres strictly to ethical guidelines concerning the responsible use of natural resources. No ethical conflicts or concerns related to human or animal welfare are present in this work.

CRediT authorship contribution statement

Manhal Gobara Hamid: Writing – original draft, Methodology, Data curation. **Khitma A. Sir Elkhatim:** Methodology, Data curation. **Amro B. Hassan:** Writing – review & editing. **Mohamed A Ibraheem:** Methodology. **Yousif M.A. Idris:** Writing – review & editing. **Faraz Muneer:** Writing – review & editing, Funding acquisition. **Mohammed Elsafy:** Writing – review & editing, Visualization, Validation, Software, Formal analysis. **Mahbubjon Rahmatov:** Writing – review & editing, Funding acquisition. **Eva Johansson:** Writing – review & editing, Visualization, Supervision, Funding acquisition. **Tilal Abdelhalim:** Writing – review & editing, Visualization, Validation, Supervision, Funding acquisition, Conceptualization.

Declaration of competing interest

The authors declare that they have no known competing financial interests or personal relationships that could have appeared to influence the work reported in this paper.

Acknowledgments

We gratefully acknowledge the financial support the Swedish Research Council (Vetenskapsrådet) provided through grant number DR. 2021-05090. We sincerely thank Vetenskapsrådet for their commitment to supporting scientific research.

Supplementary materials

Supplementary material associated with this article can be found, in the online version, at doi:10.1016/j.afres.2025.100969.

Data availability

Data will be made available on request.

References

Abdalla, A., El Tinay, A., Mohamed, B., & Abdalla, A. (1998). Proximate composition, starch, phytate and mineral contents of 10 pearl millet genotypes. *Food Chemistry, 63*(2), 243–246.

Abdalla, A. A., Ahmed, U. M., Ahmed, A. R., El Tinay, A., & Ibrahim, K. A. (2009). Physicochemical characterization of traditionally extracted pearl millet starch (Jir). *The Journal of Applied Sciences Research, 5*(11), 2016–2027.

Abebe, W., Collar, C., & Ronda, F. (2015). Impact of variety type and particle size distribution on starch enzymatic hydrolysis and functional properties of tef flours. *Carbohydrate Polymers, 115*, 260–268.

Adeyemi, I. A., & Beckley, O. (1986). Effect of period of maize fermentation and souring on chemical properties and amylograph pasting viscosity of ogi. *Journal of Cereal Science, 4*(4), 353–360.

Agama-Acevedo, E., Rodriguez-Ambriz, S. L., García-Suárez, F. J., Gutierrez-Méraz, F., Pacheco-Vargas, G., & Bello-Pérez, L. A. (2014). Starch isolation and partial characterization of commercial cooking and dessert banana cultivars growing in Mexico. *Starch-Stärke, 66*(3-4), 337–344.

Alegria, C., Pinheiro, J., Duthoit, M., Gonçalves, E. M., Moldão-Martins, M., & Abreu, M. (2012). Fresh-cut carrot (cv. Nantes) quality as affected by abiotic stress (heat shock and UV-C irradiation) pre-treatments. *LWT-Food Science and Technology, 48*(2), 197–203.

Ali, M. A., El Tinay, A. H., & Abdalla, A. H. (2003). Effect of fermentation on the in vitro protein digestibility of pearl millet. *Food Chemistry, 80*(1), 51–54.

Aloys, N., & Zhou, H. M. (2006). Functional and chemical properties of Ikivunde and Inyange, two traditionally processed Burundian cassava flours. *Journal of Food Biochemistry, 30*(4), 429–443.

Bankole, Y., Tanimola, O., Odunukan, R., & Samuel, D. (2013). An assessment of the functional properties, proximate composition, sensory evaluation and Rheological value of Gari fortified with bambara groundnut flour (Voandzeia Subterranean Thouars). *International Letters of Natural Sciences, 1*.

Bian, X., Chen, J.r., Yang, Y., Yu, D.h., Ma, Z.q., Ren, L.k., Wu, N., Chen, F.l., Liu, X.f., Wang, B., & Zhang, N. (2022). Effects of fermentation on the structure and physical properties of glutinous proso millet starch. *Food Hydrocolloids, 123*, Article 107144. https://doi.org/10.1016/j.foodhyd.2021.107144

Chandrasekar, V., Nambi, E. V., Sultan, S., & John, S. G. (2022). Effect of operating conditions of a solid-state fermenter on structural and pasting properties of finger millet flour as applied to bread quality. *Journal of Food Process Engineering, 45*(5), Article e14017.

Chauhan, D., Gujral, H. S., Perera, D., & Dhital, S. (2024). Flaking of millets and its impact on bioactivity, pasting, digestibility, structural and thermal properties. *Food Chemistry, 458*, Article 140240.

Chávez-Murillo, C. E., Wang, Y. J., Quintero-Gutierrez, A. G., & Bello-Pérez, L. A. (2011). Physicochemical, textural, and nutritional characterization of Mexican rice cultivars. *Cereal Chemistry, 88*(3), 245–252.

Cobb, B., & Schoelles, D. (1989). Rapid method for determining amylose using a microplate reader. *HortScience : A Publication of the American Society for Horticultural Science, 24*(3), 487–488.

Correia, P. R., Nunes, M. C., & Beirão-da-Costa, M. L. (2013). The effect of starch isolation method on physical and functional properties of Portuguese nut starches. II. Q. rotundifolia Lam. and Q. suber Lam. acorns starches. *Food Hydrocolloids, 30*(1), 448–455. https://doi.org/10.1016/j.foodhyd.2012.06.014

Dang, J. M. C., & Copeland, L. (2004). Genotype and environmental influences on pasting properties of rice flour. *Cereal Chemistry, 81*(4), 486–489.

Dirar, H. A. (1993). *The indigenous fermented foods of the Sudan: A study in African food and nutrition*.

Dirar, H. A. (1994). Commentary: The fermented foods of the Sudan.

Elsafy, M., Othman, M. H., Hassan, A. B., Elkhatim, K. A. S., Hamid, M. G., Rahmatov, M., & Abdelhalim, T. S. (2024). Phytochemical components and antioxidant properties of traditional Sudanese pearl millet nonalcoholic drink. *Food Chemistry Advances*, Article 100739.

Giuberti, G., Marti, A., Gallo, A., Grassi, S., & Spigno, G. (2019). Resistant starch from isolated white sorghum starch: Functional and physicochemical properties and resistant starch retention after cooking. A comparative study. *Starch-Stärke, 71*(7-8), Article 1800194.

Gong, S., Xie, F., Lan, X., Zhang, W., Gu, X., & Wang, Z. (2020). Effects of fermentation on compositions, color, and functional properties of gelatinized potato flours. *Journal of Food Science, 85*(1), 57–64.

Gupta, R., & Gaur, S. (2024a). Investigating the effect of natural fermentation in modifying the physico-functional, structural and thermal characteristics of pearl and finger millet starch. *Journal of the Science of Food and Agriculture, 104*(4), 2440–2448. https://doi.org/10.1002/jsfa.13129

Gupta, R., & Gaur, S. (2024b). Investigating the effect of natural fermentation in modifying the physico-functional, structural and thermal characteristics of pearl and finger millet starch. *Journal of the Science of Food and Agriculture, 104*(4), 2440–2448.

Hamid, M. G., Sir Elkhatim, K. A., Idris, Y. M. A., Elsafy, M., Rahmatov, M., Abdelhalim, T., & Muneer, F. (2025). Impact of fermentation time on the in vitro enzymatic digestibility of traditionally extracted pearl millet (Pennisetum glaucum) starch. *LWT, 218*, Article 117523. https://doi.org/10.1016/j.lwt.2025.117523

Hong, J., Guo, W., Chen, P., Liu, C., Wei, J., Zheng, X., & Saeed Omer, S. H. (2022). Effects of bifidobacteria fermentation on physico-chemical, thermal and structural properties of wheat starch. *Foods), 11*(17), 2585.

Ilowefah, M., Bakar, J., Ghazali, H. M., Mediani, A., & Muhammad, K. (2015). Physicochemical and functional properties of yeast fermented brown rice flour. *Journal of Food Science and Technology, 52*, 5534–5545.

Im, H.S., You, G.S., Jung, Y.H., & Shin, H.J. (2023). Recent research trends in mushroom mycelium-based materials.

Juliano, B. O. (1971). A simplified assay for milled-rice amylose. *Cereal Science Today, 12*, 334–360.

Kaur, M., Sandhu, K. S., & Lim, S. T. (2010). Microstructure, physicochemical properties and in vitro digestibility of starches from different Indian lentil (Lens culinaris) cultivars. *Carbohydrate Polymers, 79*(2), 349–355. https://doi.org/10.1016/j.carbpol.2009.08.017

Kim, S. H., Lee, B. H., Baik, M. Y., Joo, M. H., & Yoo, S. H. (2007). Chemical structure and physical properties of mung bean starches isolated from 5 domestic cultivars. *Journal of Food Science, 72*(9), C471–C477.

Kumar, A., Tripathi, M. K., Joshi, D., & Kumar, V. (2021). *Millets and millet technology*. Springer.

Li, Y., Cheng, X., Shi, F., Wang, L., Li, Y., & Chen, Z. (2019). Effect of solid-state fermentation by lactobacillus plantarum on the cooking quality, microstructure, and physicochemical properties of brown rice. *Starch-Stärke, 71*(3-4), Article 1800160.

Lin, C., & Zayas, J. (1987). Functionality of defatted corn germ proteins in a model system: Fat binding capacity and water retention. *Journal of Food Science, 52*(5), 1308–1311.

Maskan, M. (2001). Kinetics of colour change of kiwifruits during hot air and microwave drying. *Journal Of Food Engineering, 48*(2), 169–175.

McDermott, E. (1980). The rapid non-enzymic determination of damaged starch in flour. *Journal of the Science of Food and Agriculture, 31*(4), 405–413.

Mohamed, A. A., Alamri, M. S., Hussain, S., Ibraheem, M. A., & Qasem, A. A. (2019). Rheological properties of sweet potato starch-date syrup gel. *Food Science and Technology, 39*, 1030–1039.

Obadina, A. O., Fegha, G. D., & Olugbile, A. O. (2013). Effect of fermentation periods on chemical and physicochemical properties of cocoyam starch. *Starch-Stärke, 65*(9-10), 747–752.

Osungbaro, T. O. (1990). Effect of fermentation period on amylose content and textural characteristics of "Ogi"(a fermented maize porridge). *Journal of Fermentation and Bioengineering, 70*(1), 22–25.

Owuamanam, C., Iwouno, J., Ihediohanma, N., & Barber, L. (2010). Cyanide reduction, functional and sensory quality of gari as affected by pH, temperature and fermentation time. *Pakistan Journal of Nutrition, 9*(10), 980–986.

Purewal, S. S., Siroha, A. K., Salar, R. K., Kaur, A., Singh, R. S., Kennedy, J. F., & Bangar, S. P. (2024). Influence of solid-state fermentation on the functional characteristics of pearl millet starch: An innovative and cost-efficient approach to modify starch. *Carbohydrate Polymer Technologies and Applications, 7*, Article 100449.

Samah, K., & Muna, A. (2011). Jir hur a Fermented Millet (Penisitum typhoidism) Product of Sudan.

Sandhu, K. S., Singh, N., & Kaur, M. (2004). Characteristics of the different corn types and their grain fractions: Physicochemical, thermal, morphological, and rheological properties of starches. *Journal of Food Engineering, 64*(1), 119–127. https://doi.org/10.1016/j.jfoodeng.2003.09.023

Sandhu, K. S., & Siroha, A. K. (2017). Relationships between physicochemical, thermal, rheological and in vitro digestibility properties of starches from pearl millet cultivars. *LWT - Food Science and Technology, 83*, 213–224. https://doi.org/10.1016/j.lwt.2017.05.015

Serba, D. D., Yadav, R. S., Varshney, R. K., Gupta, S., Mahalingam, G., Srivastava, R. K., Gupta, R., Perumal, R., & Tesso, T. T. (2020). Genomic designing of pearl millet: A resilient crop for arid and semi-arid environments. *Genomic Designing Of Climate-Smart Cereal Crops*, 221–286.

Tonapi, V. A., Thirunavukkarasu, N., Gupta, S., Gangashetty, P. I., & Yadav, O. (2024). *Pearl Millet in the 21st Century*. Springer.

Vidal, N. P., Manful, C. F., Pham, T. H., Stewart, P., Keough, D., & Thomas, R. (2020). The use of XLSTAT in conducting principal component analysis (PCA) when evaluating the relationships between sensory and quality attributes in grilled foods. *MethodsX, 7*, Article 100835.

Wang, J., & Kinsella, J. (1976). Functional properties of novel proteins: Alfalfa leaf protein. *Journal of Food Science, 41*(2), 286–292.

Williams, P. (1970). A rapid colorimetric procedure for estimating the amylose content of starches and flours. *Cereal chemistry, 47*, 411–420.

Wu, D., Ma, H., Fu, M., & Tang, X. (2022). Insight into multi-scale structural evolution during gelatinization process of normal and waxy maize starch. *Journal of Food Science And Technology, 59*(11), 4405–4414.

Yousaf, L., Hou, D., Liaqat, H., & Shen, Q. (2021). Millet: A review of its nutritional and functional changes during processing. *Food Research International, 142*, Article 110197.

Zhao, T., Li, X., Zhu, R., Ma, Z., Liu, L., Wang, X., & Hu, X. (2019). Effect of natural fermentation on the structure and physicochemical properties of wheat starch. *Carbohydrate Polymers, 218*, 163–169. https://doi.org/10.1016/j.carbpol.2019.04.061